Middle Rio Grande Physical Modeling

Assessment of equations for predicting flow velocities associated with transverse features using field data from the Bernalillo river maintenance site on the Middle Rio Grande

Amanda L. Cox, S. Michael Scurlock, Christopher I. Thornton, and Steven R. Abt

Peer Technical Review by Drew C. Baird, Bureau of Reclamation, Denver Technical Service Center, Denver Colorado

August 2012

Colorado State University
Engineering Research Center
Department of Civil and Environmental Engineering

Middle Rio Grande Physical Modeling

Assessment of equations for predicting flow velocities associated with transverse features using field data from the Bernalillo river maintenance site on the Middle Rio Grande

Prepared by:

Colorado State University
Daryl B. Simons Building at the
Engineering Research Center
Fort Collins, Colorado 80523

Prepared for:

U.S. Department of the Interior
Bureau of Reclamation
Albuquerque Area Office
555 Broadway N.E., Suite 100
Albuquerque, New Mexico 87102-2352

This research has been completed at Colorado State University with funding from the U. S. Bureau of Reclamation in Albuquerque, NM, via U. S. Forest Service Contract: 07-JV-221602-264. This research was supported in part by funds provided by the Rocky Mountain Research Station, Forest Service, U. S. Department of Agriculture.

Table of Contents

List of Figures

List of Tables

Executive Summary

In-stream transverse features were identified by the Bureau of Reclamation (Reclamation) as potential solutions to lateral channel instability in the Middle Rio Grande downstream of Cochiti Dam. Reclamation contracted with Colorado State University to conduct physical model studies to evaluate hydraulic effects of transverse structures and to develop design procedures to quantify the hydraulic effects. A result of this effort was the development of a suite of empirical equations to predict changes in flow velocities along the centerline, inner-bank, and outer-bank of a channel bend for different types of transverse structures (Scurlock *et al.* 2012). Previously, limited guidelines were available to determine hydraulic conditions associated with transverse features; and implemented designs had largely been based on engineering judgment and lacked physically-based design criteria (Scurlock *et al*. 2012b; Radspinner *et al.* 2010).

The Scurlock *et al.* (2012b) equations predict ratios of maximum or average flow velocities along a channel with installed transverse features to baseline (pre-structure installation) cross-sectional averaged velocities. The resulting ratios were termed Maximum Velocity Ratio (*MVR*) and Average Velocity Ratio (*AVR*) with subscripts *o*, *c*, and *i* denoting outer-bank, centerline, and inner-bank locations, respectively. Velocity-ratio prediction equations were developed by Scurlock *et al.* (2012b) for spur dikes, submerged spur dikes, and vanes. Additionally, one set of equations was developed that encompassed all three types of transverse-feature structures. The current investigation utilized data from a field site with installed bendway weirs to provide an assessment of the velocity-ratio equations. This assessment serves to bridge the gap from laboratory data to field applications and is intended to aid in future development of effective design equations and methods.

Reclamation constructed a series of bendway weirs in 2007 to mitigate lateral channel migration at the Bernalillo Priority Site of the Middle Rio Grande in New Mexico. Parameters required for computing *MVR* and *AVR* values at the Bernalillo Site were obtained from field data, the final design report and drawings, and aerial photographs. Velocity field data collected near the bendway weir structures by Reclamation in 2007 and 2008 were used to compute observed *MVR* and *AVR* values; and representative baseline flow velocities and other hydraulic parameters were obtained using a Hydrologic Engineering Centers River Analysis System (HEC-RAS) model of the Bernalillo Site.

Velocity ratios were predicted for the Bernalillo Site along the channel centerline and outer-bank using the equations for all structures, vanes, and submerged spur dikes. The submerged spur dike equations were collectively the best predictor for AVR_o, MVR_c, and AVR_c; and the all-structures equation was the best predictor for MVR_o. Twenty of the twenty-four total computed velocity ratios were within expected ranges regardless of multiple field parameters falling outside the bounds of the dataset from which the prediction equations were developed. Additionally, nearly all computed *MVR* values (83%) were greater than corresponding *AVR* values, indicating continuity between the set of prediction equations.

Field-data limitations required using multiple assumptions to complete the analysis, which contribute to uncertainty in computed velocity ratios. The lack of baseline channel geometry data and corresponding hydraulic conditions induces the most uncertainty in the analysis. Additionally, as-built surveys of the structures were not available which required estimating some of the analysis parameters from final designs and limited cross section surveys. Despite field-data limitations, the assessment of the *MVR* and *AVR* equations was productive and identified that the required inputs could be easily attainable from a transverse-feature design. To

provide a highly quantitative assessment of the Scurlock *et al.* (2012b) velocity-ratio prediction methods, a field study specifically designed to capture information for assessing the velocity-ratio equations is recommended.

Introduction

Transverse in-stream structures can provide valuable river training benefits including protection from channel erosion and lateral migration (Radspinner *et al.* 2010). Transverse structures are deflector structures that extend from one bank into the channel without reaching the other side (Shields 1983). For transverse structures, bank erosion protection is accomplished by controlling near-bank flow velocities and shear stresses. The Albuquerque Area Office of the Bureau of Reclamation (Reclamation) identified transverse structures as potential solutions to channel instability in the Middle Rio Grande downstream of Cochiti Dam. The Middle Rio Grande was historically classified as a perennial braided stream. In 1973, Cochiti Dam was built to provide flood control and sediment detention for the Albuquerque area. As a result, the dam traps nearly all the sediment supplied by a 14,600-mi^2 watershed (Richard 2001). Due to substantial reservoir sedimentation and the consequential sediment deficit of the Middle Rio Grande, an alteration in planform occurred. Richard (2001) stated that, in general, the channel transformed from a braided channel to a meandering stream containing a pool-riffle sequence with coarse-gravel substrate. Prior to 1970, two large tributaries to the Middle Rio Grande (Galisteo Creek and the Jemez River) were dammed, which further contributed to the sediment deficiency (Schmidt 2005).

Lateral migration caused by the change in morphology marginalized riverside infrastructure and reduced riparian vegetation and aquatic habitat (Heintz 2002). In an effort to protect riverside infrastructure, Reclamation implemented a channel maintenance program to stabilize the channel with an additional goal of improving aquatic habitat. Traditional methods of bank stabilization such as riprap revetment and concrete structures are not aesthetically pleasing and do not promote aquatic habitat or riparian vegetation. Alternative methods such as transverse structures have proven to stabilize banks and increase aquatic habitat (Davinroy *et al.* 1998, Derrick 1998, Shields *et al.* 1998). Although transverse features have been identified to be a suitable alternative to traditional methods, limited design guidelines are available that address how these structures effect hydraulic conditions within the channel (Scurlock *et al.* 2012b). Previously implemented designs have largely been based on engineering judgment and lacked physically-based design criteria (Scurlock *et al.* 2012b; Radspinner *et al.* 2010).

Reclamation contracted with Colorado State University to conduct physical model studies to evaluate hydraulic effects of transverse structures and to develop design procedures to quantify the hydraulic effects. A 1:12 rigid-bed physical model was constructed in 2001 and hydraulic data were collected for 130 unique transverse-structure installations (Heintz 2002, Darrow 2004, Schmidt 2005, Scurlock *et al.* 2012b). Two prismatic, trapezoidal channel bends were originally constructed in the physical model as scaled representations of the study reaches within the Middle Rio Grande River near Albuquerque, New Mexico. Scurlock *et al.* (2012b) developed a suite of empirical equations to predict changes in flow velocities along the centerline, inner-bank, and outer-bank of a channel bend for different types of transverse structures.

In 2007, Reclamation constructed a series of bendway weirs at the Bernalillo Priority Site of the Middle Rio Grande to mitigate lateral channel migration (Sixta and Nemeth 2005; BIO-WEST 2005). Figure 1 identifies the location of the Bernalillo Priority Site which is located on the east side of the Rio Grande, approximately 3,300 ft south of the U. S. Highway 550 bridge in Bernalillo. In 2007 and 2008, flow-velocity measurements within the Bernalillo Priority Site weir field were collected in addition to cross-section surveys and discharge measurements (Bui

2011, Baird 2012). The objectives of the current investigation are to review the Bernalillo Priority Site field data and utilize the field data to provide an assessment of the velocity equations developed by Scurlock *et al.* (2012b). This assessment serves to bridge the gap from laboratory data to field applications and is intended to aid in future development of effective design equations and methods.

Figure 1. Bernalillo Priority Site location

Velocity-ratio Prediction Equations

Scurlock *et al.* (2012b) provided equations for predicting changes in flow velocities along the centerline, inner-bank, and outer-bank of a channel bend for different types of transverse structures. Heintz (2002) originally defined the concept of the maximum velocity ratio (*MVR*) as the ratio of the maximum velocity magnitude observed within a structure field (*MV*) to the baseline cross-section mean velocity averaged through the bend along the thalweg direction ($V_{AveBaseline}$):

$$MVR = \frac{MV}{V_{Ave\ Baseline}} \tag{1}$$

In addition to investigating the maximum velocity ratio, Scurlock *et al.* (2012b) defined the bend-averaged velocity ratio (*AVR*) as the ratio of the bend-averaged velocity magnitude measured within a structure field (*AV*) to the baseline cross-section averaged velocity along the thalweg direction ($V_{AveBaseline}$):

$$AVR = \frac{AV}{V_{Ave\ Baseline}} \tag{2}$$

Scurlock *et al.* (2012b) identified influential structure and flow parameters affecting *MVR* and *AVR*, organized the parameters into dimensionless groupings, and developed Equation (3) for the evaluation of the velocity ratios:

$$MVR, AVR = a_1 (A^*)^{a_2} \left(\frac{L_{ARC}}{T_W}\right)^{a_3} \left(\frac{R_C}{T_W}\right)^{a_4} \left(\frac{L_{W-PROJ}}{T_W}\right)^{a_5} \left(\frac{D_B}{D_B - \Delta z}\right)^{a_6} \left(\frac{2\theta}{\pi}\right)^{a_7} \tag{3}$$

where:

A^*	=	ratio of projected cross-sectional weir area to baseline cross-sectional flow area at design flow;
$L_{W\text{-}PROJ}$	=	projected length of structure into channel (length of the weir crest Lw *sin θ) [L];
L_{ARC}	=	arc length between centerline of structures [L];
R_C	=	radius of curvature of channel bend centerline [L];
T_W	=	averaged top width of channel measured at baseline in bend [L];
D_B	=	averaged maximum cross-section baseline flow depth in bend [L];
Δz	=	elevation difference between water surface and structure crest [L];
θ	=	structure plan angle [radians]; and
$a_1, \ldots, a_7$	=	regression coefficients.

The dimensionless terms in Equation (3) can be interpreted (left to right) as an area contraction ratio, a structure spacing ratio, a curvature ratio, a lateral contraction ratio, a vertical contraction ratio, and a normalized structure planform angle. Due to the dimensionless parameters, Equation (3) is independent of scale and system of units as long as consistency is maintained (Scurlock *et al.* 2012b). Figure 2 provides a plan view and Figure 3 provides a profile view of transverse structures installed in a trapezoidal model with geometric parameter terms identified.

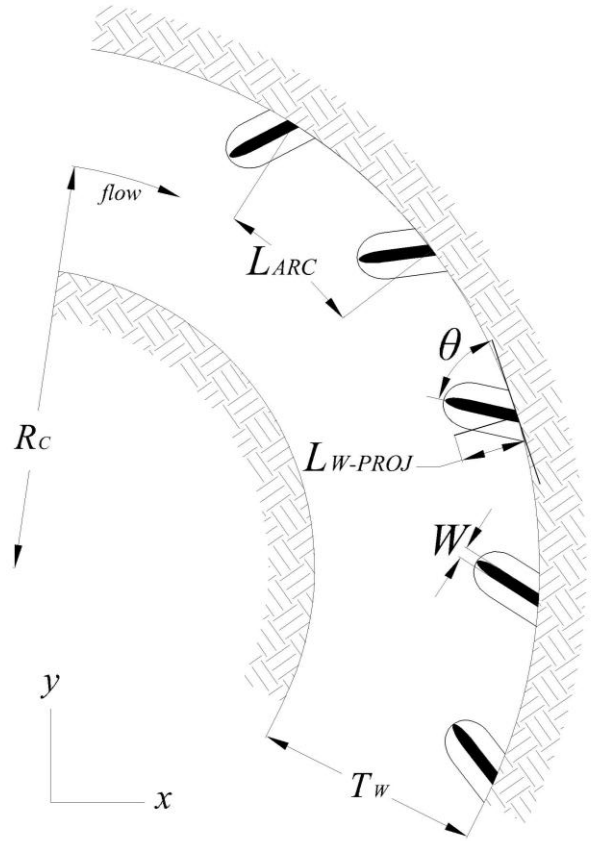

Figure 2. Plan-view schematic of parameters in Equation (3) (from Scurlock *et al.* (2012b))

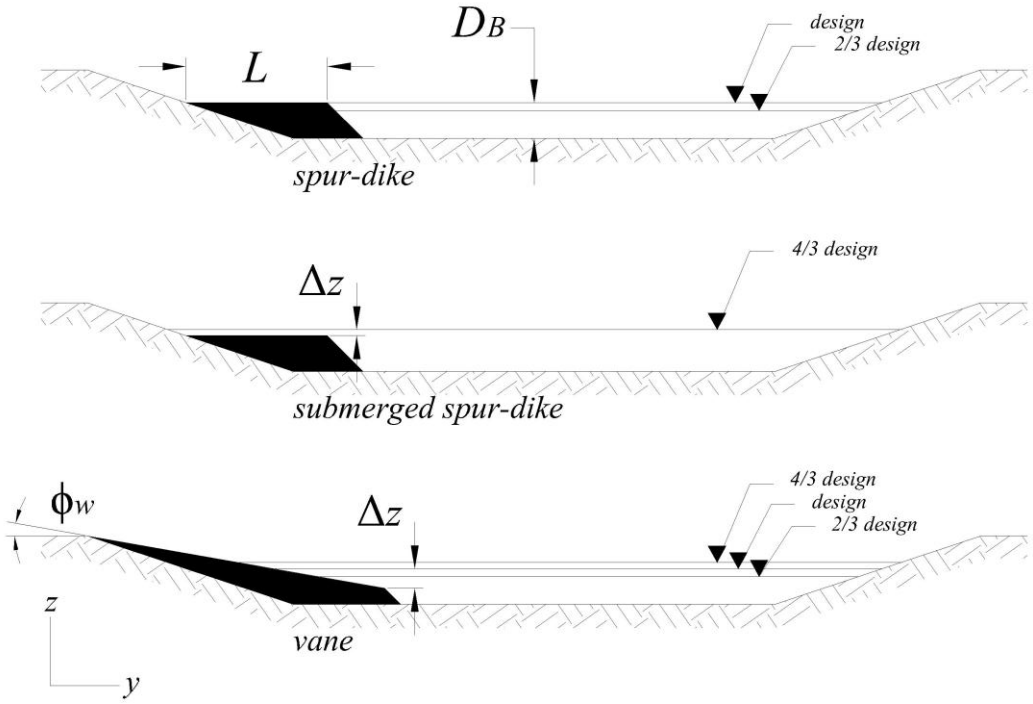

Figure 3. Profile-view schematic of parameters in Equation (3) (from Scurlock *et al.* (2012b))

Scurlock *et al.* (2012b) presented twenty-four unique design equations based on Equation (3) for induced structure hydraulics associated with spur-dikes, vanes, submerged spur dikes, and the combined structure set. Figure 3 illustrates the geometric differences between the three structure types tested. Spur dikes have a horizontal crest set at bankfull elevation; vanes have a sloped crest height that intersects the bank at or above bankfull elevation; and submerged spur dikes have a submerged horizontal crest. Submerged spur dikes were identified in the physical modeling by spur-dike configurations in which the water-surface elevation was greater than the weir-crest elevation (Scurlock *et al.* 2012b). Regression coefficients a_1 through a_7, at the outer-bank, centerline, and inner-bank (subscripts, *o*, *c*, *i*, respectively), for each of the structure sets are presented in Table 1 along with the coefficient of determination (R^2) and the mean absolute percent error (*MA%E*).

Table 1. Coefficients for *MVR* and *AVR* regression equations

All Data (130)									
Ratio Location	R^2	*MA%E*	a_1	a_2	a_3	a_4	a_5	a_6	a_7
MVR_o	0.8429	20.8533	0.0068	0.0000	0.5546	0.3846	-2.1431	0.7003	0.3824
MVR_c	0.8011	4.3100	0.3773	0.2695	0.0000	0.1973	-0.1563	0.0467	0.1155
MVR_i	0.6087	4.4433	0.3400	0.3404	-0.1116	0.1065	-0.2084	0.0445	0.1580
AVR_o	0.4861	40.7230	0.0138	0.0000	0.5917	0.7439	-1.1451	0.4629	0.5996
AVR_c	0.7255	4.0327	0.3615	0.2710	-0.0739	0.1850	-0.1412	0.0536	0.1158
AVR_i	0.7530	3.9452	0.1315	0.4894	-0.1308	0.1770	-0.4098	0.1170	0.1266
Spur Dike (60)									
Ratio Location	R^2	*MA%E*	a_1	a_2	a_3	a_4	a_5	a_6	a_7
MVR_o	0.8317	20.7074	5.648E-11	3.5354	1.1335	0.0000	-7.8000	-1.9823	0.5963
MVR_c	0.9014	3.2235	1.7160	0.0000	-0.0881	0.2674	0.3711	0.1581	0.1970
MVR_i	0.6215	4.9464	2.1970	0.0000	-0.0434	0.0000	0.2684	0.2087	0.2253
AVR_o	0.7305	28.5942	4.175E-11	3.5645	1.0828	0.0000	-7.5607	-2.1849	0.0000
AVR_c	0.7914	3.3918	1.7267	0.0000	-0.1023	0.1758	0.3473	0.1971	0.2053
AVR_i	0.7876	3.6910	1.9293	0.0000	-0.1468	0.1512	0.3831	0.4048	0.1835
Vane (40)									
Ratio Location	R^2	*MA%E*	a_1	a_2	a_3	a_4	a_5	a_6	a_7
MVR_o	0.8865	15.7708	9.332E-09	4.1556	0.0000	-0.4323	-5.0082	0.0000	0.5037
MVR_c	0.7346	3.1619	0.2301	0.5052	0.0000	0.0000	-2.9864	-0.0592	0.0000
MVR_i	0.5455	2.9724	0.3289	0.3993	-0.0603	0.0000	-0.2279	0.0000	0.0000
AVR_o	0.3246	50.8338	0.0004	1.3130	-1.9376	2.2401	0.0000	0.0000	1.0996
AVR_c	0.6645	3.2535	0.2285	0.4704	0.0000	0.0000	-0.3073	-0.0336	0.0000
AVR_i	0.7740	2.4986	0.0313	1.1117	0.0000	-0.2800	-0.7970	-0.1123	0.0000
Submerged Spur Dike (30)									
Ratio Location	R^2	*MA%E*	a_1	a_2	a_3	a_4	a_5	a_6	a_7
MVR_o	0.9535	9.2943	5.396E-10	3.0887	0.8140	0.0000	-7.0740	0.0000	0.0000
MVR_c	0.9048	3.4581	1.4770	0.0000	0.0000	0.2457	0.2287	0.0000	0.1971
MVR_i	0.8103	2.7650	1.8839	0.0000	0.0000	0.0663	0.2059	0.0000	0.2312
AVR_o	0.8630	16.1133	0.0073	0.0000	0.7710	0.0000	-2.1743	0.0000	0.0000
AVR_c	0.8966	2.4299	0.7546	0.1147	0.0000	0.1529	0.0000	0.0000	0.2002
AVR_i	0.8278	3.1874	1.6875	0.0000	0.0000	0.1024	0.2276	0.0000	0.1859

Prior to the Scurlock *et al.* (2012b) velocity-ratio prediction equations, Scurlock *et al.* (2012a) provided MVR_o best-fit and envelope velocity-ratio equations of natural-logarithmic form developed using data from all physically-modeled structures. Equation (4) provides the Scurlock *et al.* (2012a) best-fit equation for computing velocity ratios along the outer bank, and Equation (5) provides the envelope regression equation:

$$MVR_0 = -1.3917 + 0.2242\ln\left(\frac{L_{ARC}}{T_W}\right) + 0.1977\ln\left(\frac{R_C}{T_W}\right) - 0.9590\ln\left(\frac{L_{W-PROJ}}{T_W}\right) + 0.3018\ln\left(\frac{D_B}{D_B - \Delta z}\right) + 0.1657\ln\left(\frac{2\theta}{\pi}\right) \quad (4)$$

$$MVR = -1.2124 + 0.2242\ln\left(\frac{L_{ARC}}{T_W}\right) + 0.1977\ln\left(\frac{R_C}{T_W}\right) - 0.9590\ln\left(\frac{L_{W-PROJ}}{T_W}\right) + 0.3018\ln\left(\frac{D_B}{D_B - \Delta z}\right) + 0.1657\ln\left(\frac{2\theta}{\pi}\right) \quad (5)$$

Maximum outer-bank velocity ratios computed by Equation (4) and (5) were also evaluated using the Bernalillo Field site data.

Bernalillo Priority Site

As depicted in Figure 1, the Bernalillo Priority Site is located near the town of Bernalillo, New Mexico, on the east side of the Rio Grande, approximately 3,300 ft south of the U. S. Highway 550 bridge. In 2007, twelve bendway weirs were constructed at the site, four of which were intentionally buried as part of the design (BIO-WEST 2005, 2006). Figure 4 provides pre- and post-construction aerial photographs of the site; and Figure 5 provides an aerial photograph of the constructed weirs taken February 28, 2007. Prior to weir installation, the primary concern at the Bernalillo site was that the east bank of the Rio Grande was approximately 90 ft from the toe of the levee and upstream flows were directed at the east bank (Sixta and Nemeth 2005).

Figure 4. Pre-construction aerial photograph dated March 31, 2006 (left) and post-construction aerial photograph dated February 25, 2007 (right)

Figure 5. Aerial photograph of constructed bendway weirs dated February 25, 2007

Figure 6 provides a plan-view sketch of the bendway-weir field design, which includes twelve weirs with the upstream four structures intentionally buried. Table 2 provides a summary of the bendway-weir design parameters; and Figure 7 and Figure 8 provide sketches in plan view and section view, respectively, which define the design parameters (BIO-WEST 2005, 2006). Each structure is 25 ft in length oriented upstream with a planform angle (θ) of 70 degrees. Thus, the projected length into the channel ($L_{W\text{-}PROJ}$) is 23.5 ft. The arc length between the centerline of the structures (L_{ARC}) is 75.0 ft and the crest slope (S_C) is constant for all structures at 0.04 ft/ft. The channel cross-section area of the weir (A_W) was computed as 87.5 ft^2 from the weir profile geometry.

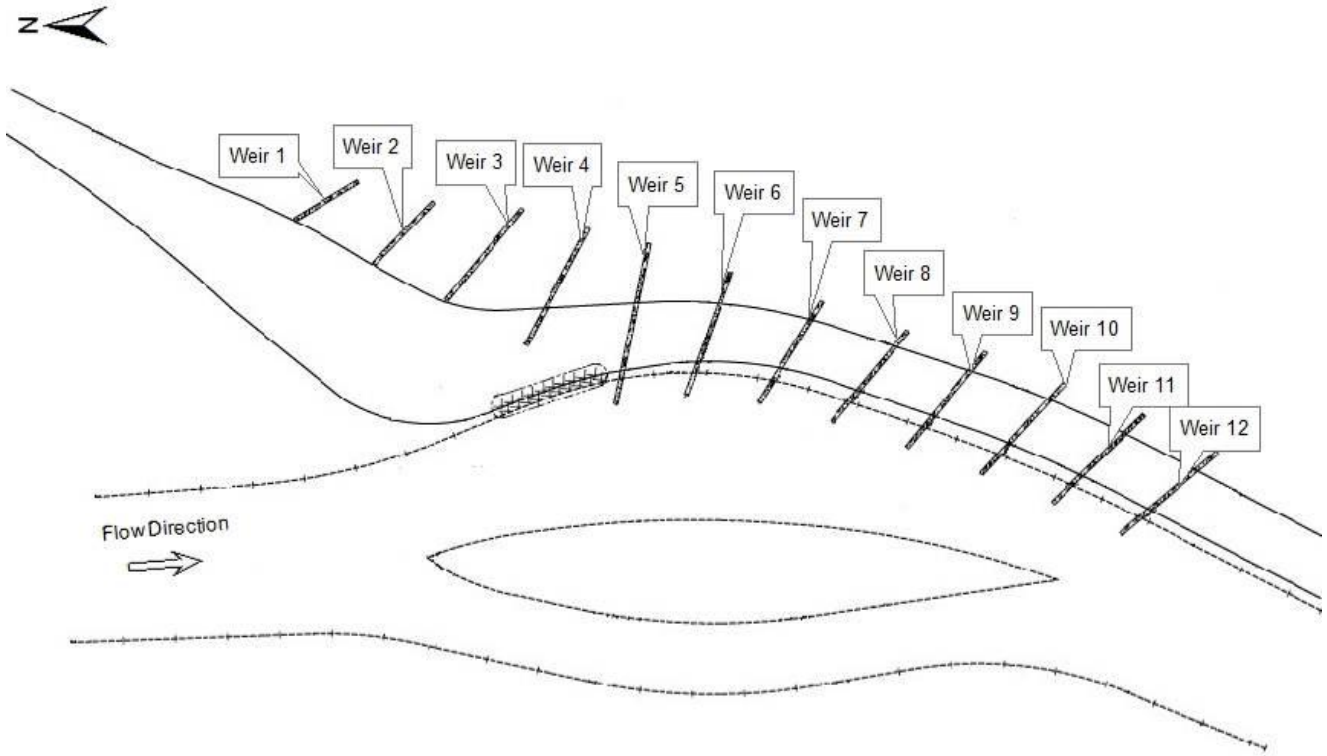

Figure 6. Plan-view sketch of bendway-weir field design (adapted from BIO-WEST (2006))

Table 2. Bendway-weir design parameters

Variable	Symbol	Value	Units
Total length of bendway weir	L_W	25.0	ft
Projected length of bendway weir into channel	$L_{W\text{-}PROJ}$	23.5	ft
Bendway-weir crest slope	S_C	0.04	ft/ft
Planform bendway-weir angle (degrees)	$\theta°$	70.0	degrees
Planform bendway-weir angle (radians)	θ	1.22	radians
Arc length (bank-line distance) between centerline of weirs	L_{ARC}	75.0	ft
Bendway-weir cross-sectional area	A_W	87.5	ft^2

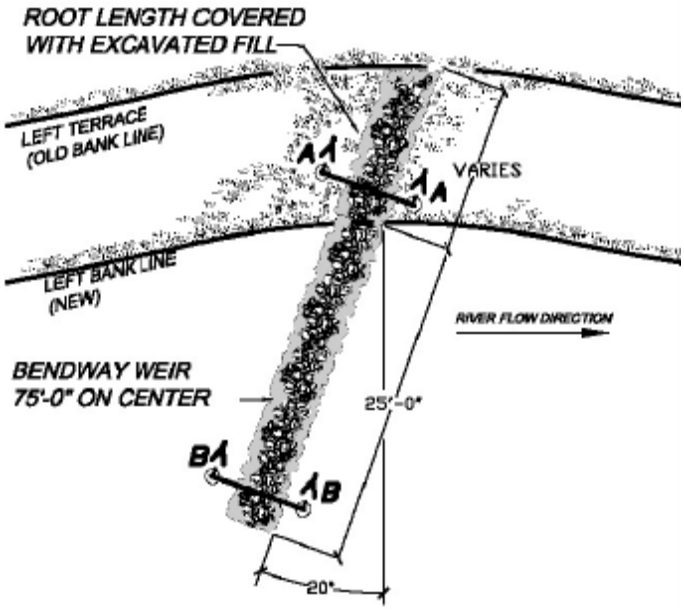

Figure 7. Bendway-weir design plan view (from BIO-WEST (2006))

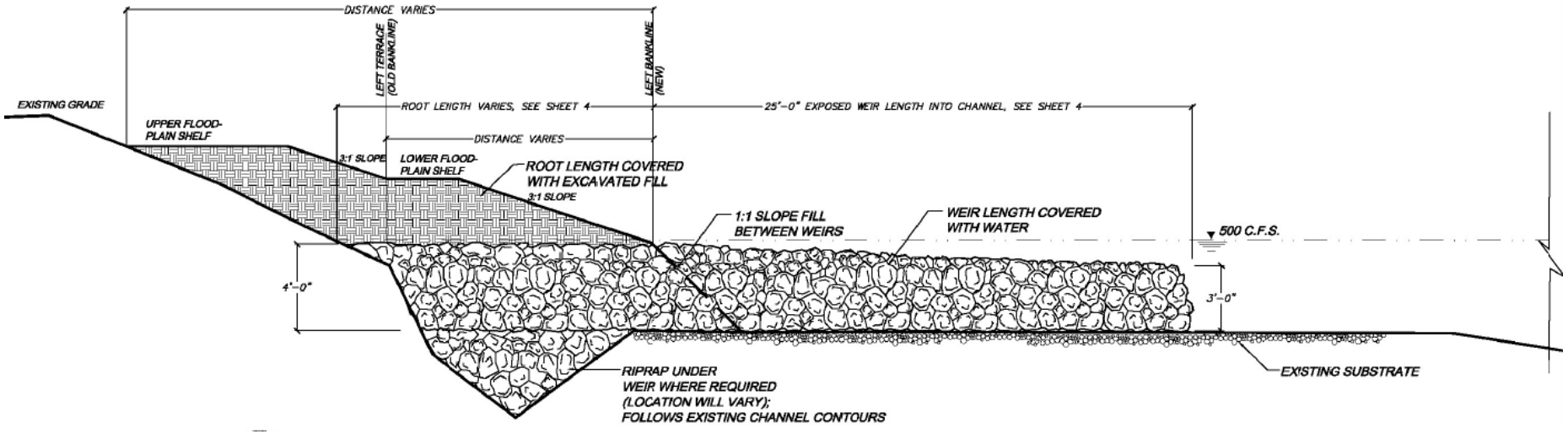

Figure 8. Bendway-weir design section view (from BIO-WEST (2006))

Field Data

Many parameters for computing *MVR* and *AVR* values at the Bernalillo Site were obtained from field data and aerial photographs. Reclamation collected cross-section surveys, discharge and velocity measurements, bed and bank material samples, and suspended sediment samples during 2007 and 2008 (Bui 2011; Baird 2012). Field data from Bui (2011) and acoustic Doppler velocimeter (ADV) data from Baird (2012) were used for evaluating the Scurlock *et al.* (2012b) *MVR* and *AVR* regression equations. Bendway-weir crest elevations were identified from cross-section surveys collected in 2007 and 2008, and channel radius of curvature was ascertained from aerial photographs. Finally, channel discharge corresponding to the times of velocity data collection were determined using measured discharge data and nearby U. S. Geological Survey (USGS) gaging stations.

Reclamation collected flow-velocity field data on May 14, 2007 using a Marsh McBirney Flow-Mate (one-dimensional velocity meter). Figure 9 illustrates the locations of velocity measurements, which included measurements around multiple weir tips and between several weirs. Measurements collected between the weirs were identified as W 1.5, W 2.5, W 3.5, W 4.5, and W 5.5; and measurements collected near the weir tips were identified as W 1-1, W 1-2, W 1-3, W 2-1, W 2-2, W 2-3, W 3-1, and W 3-2. Velocity measurements collected at W 1-2, W 2-2, and W 3-2 were used as centerline flow velocities for evaluation of the *MVR* and *AVR* equations, given their locations near the center of the channel. Flow velocities were recorded at 0.5-ft depth increments starting from 0.5 ft below the water surface for the measurement collected between the weirs and starting at 0.5 ft above the bed for the velocity measurement near the weir tips.

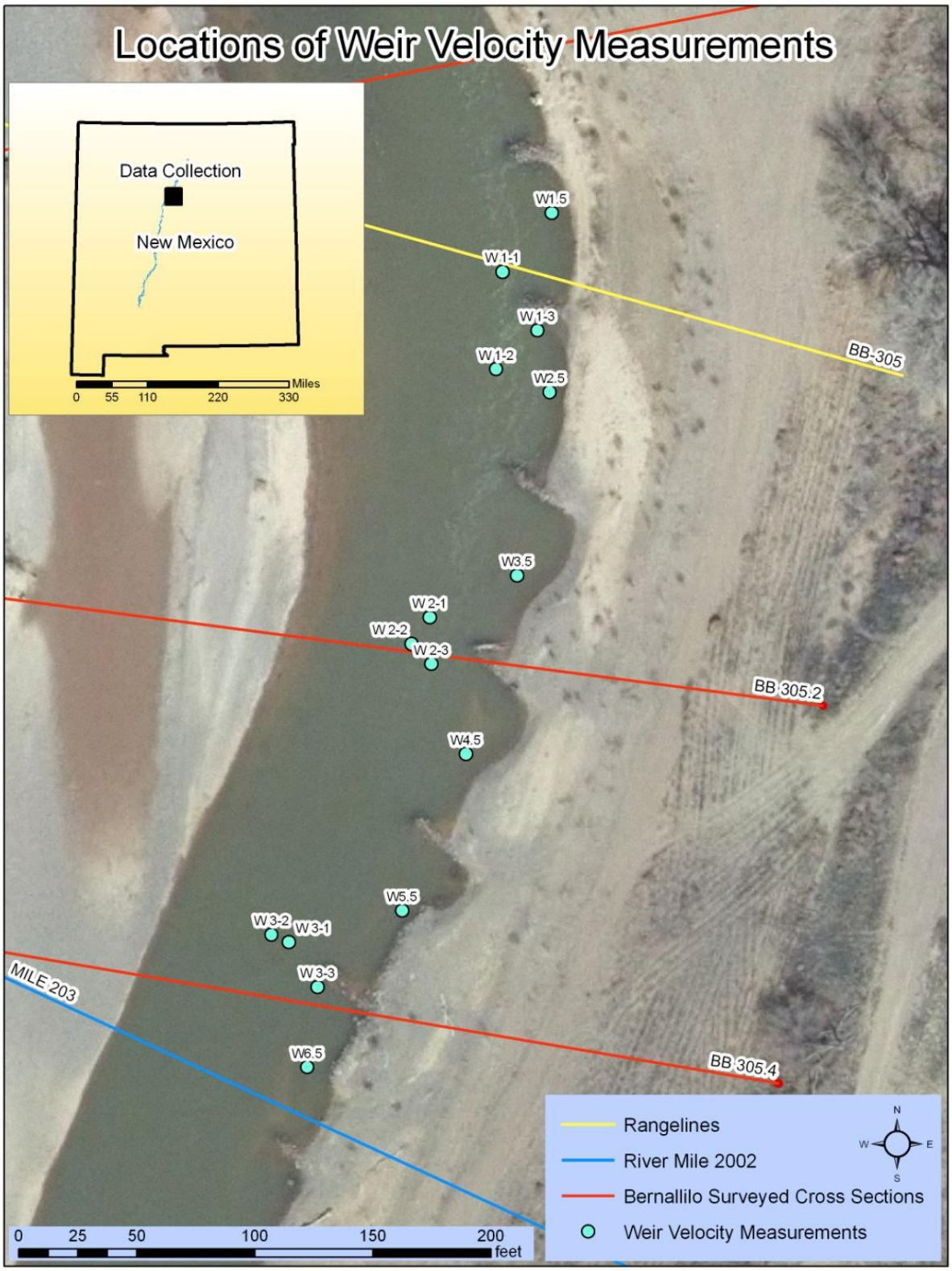

Figure 9. Locations of 2007 weir velocity measurements (from Bui (2011))

Flow velocities at 60% of the flow depth (V_{60}), as measured from the water surface, are used as an approximation for the average flow velocity within a water column for shallow flow (Buchanan and Somers 1969). Further, velocities collected at 60% of the flow depth in the physical model were used to develop the *MVR* and *AVR* equations. For evaluation of the *MVR* and *AVR* equations, the 2007 velocity field data were analyzed to determine the flow velocity at 60% of the flow depth. Using data from the W 3.5 location shown in Figure 9, Figure 10 provides an example graph of flow velocity (V_x) versus normalized distance along the flow depth (*y/D*), where *y* is the distance from the measurement location to the bed and *D* is the total flow depth. The V_{60} location corresponds to a *y/D* value of 0.40. The 60% flow velocity was computed as a linear interpolation between the data points immediately above and below 60% of the flow depth. Table 3 provides computed 60% flow velocities from the 2007 field data. The maximum and average flow velocities between the weirs (outer-bank) were 2.51 and 2.04 ft/s, respectively; and the maximum and average flow velocities along the channel centerline were 4.84 ft/s and 4.76 ft/s, respectively.

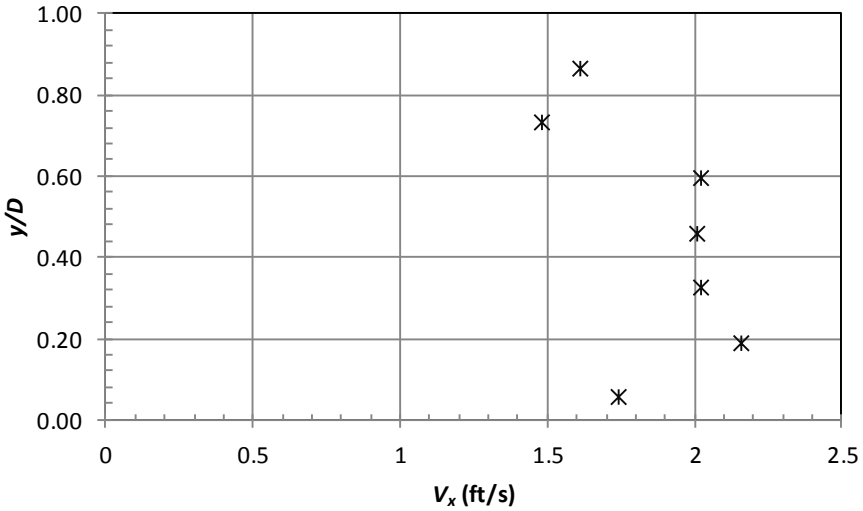

Figure 10. Vertical profile of measured flow velocities at W 3.5

Table 3. Computed 60% flow velocities from 2007 field measurements

Outer-bank Flow Velocities		
Measurement Date (mm/dd/yyyy)	Location ID	V_{60} (ft/s)
5/14/2007	W 1.5	1.74
5/14/2007	W 2.5	2.23
5/14/2007	W 3.5	2.01
5/14/2007	W 4.5	1.57
5/14/2007	W 5.5	2.17
5/14/2007	W 6.5	2.51
	Maximum Velocity:	**2.51**
	Average Velocity:	**2.04**

Centerline Flow Velocities		
Measurement Date (mm/dd/yyyy)	Location ID	V_{60} (ft/s)
5/14/2007	W 1-2	4.84
5/14/2007	W 2-2	4.64
5/14/2007	W 3-2	4.80
	Maximum Velocity:	**4.84**
	Average Velocity:	**4.76**

In addition to the 2007 velocity field data, Reclamation collected velocity field data on May 19 through May 23 of 2008 using an ADV (three-dimensional velocity meter) as reported by Baird (2012). Figure 11 illustrates the locations of velocity measurements, which included measurements 12 ft upstream and downstream of Weir 5, Weir 6, and Weir 7; 12 ft from the tips of Weir 5, Weir 6, and Weir 7; and along the bankline halfway between Weir 4 and 5, Weir 5 and 6, and Weir 6 and 7. For clarification, Weir 5 is the upstream-most weir that interacts with the flow. Weirs 1, 2, 3, and 4 were intentionally buried as part of the design. Velocity measurements collected 12 ft from the weir tips were used as centerline flow velocities for evaluation of the *MVR* and *AVR* equations, given their locations near the center of the channel. Baird (2012) analyzed the 2008 ADV velocity data to determine flow velocities at 60% of the flow depth, which were used to evaluate *MVR* and *AVR* equations for this study. Table 4 provides a summary 60% flow velocities reported in Baird (2012). The computed outer-bank velocity for the location 12 ft upstream of Weir 5 was 3.52 ft/s, which was notably greater than the 2.57 ft/s average velocity computed for the outer-bank measurements within the weir field. In the physical-model study, outer-bank velocity measurements located upstream of the upstream-most weir in the field were frequently observed to have greater flow velocities than those measured within the weir field and consequently were not used in development of the *MVR* and *AVR* equations (Scurlock *et al.* 2012b). Thus, data from the location 12 ft upstream of Weir 5 was excluded from the analysis of the *MVR* and *AVR* equations. The maximum and average flow velocities between the weirs (outer-bank) were 3.07 and 2.57 ft/s, respectively; and the maximum and average flow velocities along the channel centerline were 4.35 ft/s and 4.09 ft/s, respectively.

Figure 11. Locations of 2008 weir velocity measurement

Table 4. 60% flow velocities from 2008 ADV field measurements (from Baird (2012))

Outer-bank Flow Velocities			***Center-line Flow Velocities***		
Measurement Date (mm/dd/yyyy)	Location ID	V_{60} (ft/s)	Measurement Date (mm/dd/yyyy)	Location ID	V_{60} (ft/s)
5/19/2008	12 ft upstream of Weir 5	3.52[A]	5/21/2008	12 ft from tip of Weir 5	3.65
5/19/2008	12 ft downstream of Weir 5	2.55	5/20/2008	12 ft from tip of Weir 6	4.28
5/20/2008	12 ft upstream of Weir 6	2.59	5/20/2008	12 ft from tip of Weir 7	4.35
5/20/2008	12 ft downstream of Weir 6	2.55			
5/20/2008	12 ft upstream of Weir 7	3.07			
5/20/2008	12 ft downstream of Weir 7	2.11			
	Maximum Velocity:	**3.07**		**Maximum Velocity:**	**4.35**
	Average Velocity:	**2.57**		**Average Velocity:**	**4.09**

[A]measurement 12 ft upstream of Weir 5 was not used for evaluating *MVR* and *AVR* equations

Eight channel cross sections were surveyed in May 2007 and May 2008. Figure 12 identifies the locations of the surveyed cross sections on an aerial photograph. Cross Sections BB 304.8, BB 305.2, and BB 305.4 are located within the weir field as shown in Figure 13. Cross Section BB 305.2 was used to determine the height of the weir crest at the bank. Graphs of the 2007 and 2008 Cross Section BB 305.2 surveys are provided in Figure 14 and Figure 15, respectively. The distance between the east end of Cross Section BB 305.2 and the location where it crosses Weir 8 was determined to be approximately 130 ft using scaled images and cross-section locations. An elevation of approximately 5,048 ft was surveyed at 130 ft along Cross Section BB 305.2 for both the 2007 and 2008 survey. Additionally, the final design specified that the structure height at the bank should be set at 4 ft above the horizontal channel bed (BIO-WEST 2005). Figure 14 reveals that the channel elevation lowers to approximately 5,044 at 150 ft along Cross Section BB 305.2, which further supports the conclusion that the weir crest elevation was set at 5,048 ft. In contradiction to the post-construction surveys, the final grading plan for the site, shown in Figure 16, specifies a horizontal channel-bed section at an elevation of 5,042 ft where the weirs were to be constructed (BIO-WEST 2006). However, the 2007 cross-section surveys indicate that the channel bed elevation was constructed closer to 5,044 ft. Figure 17 and Figure 18 provide the 2007 cross-section survey graphs for Cross Sections BB 304.8 and BB 305.4, respectively, with a marker identifying the location of the channel-bed section adjacent to the weir field.

Figure 12. Cross-section survey locations

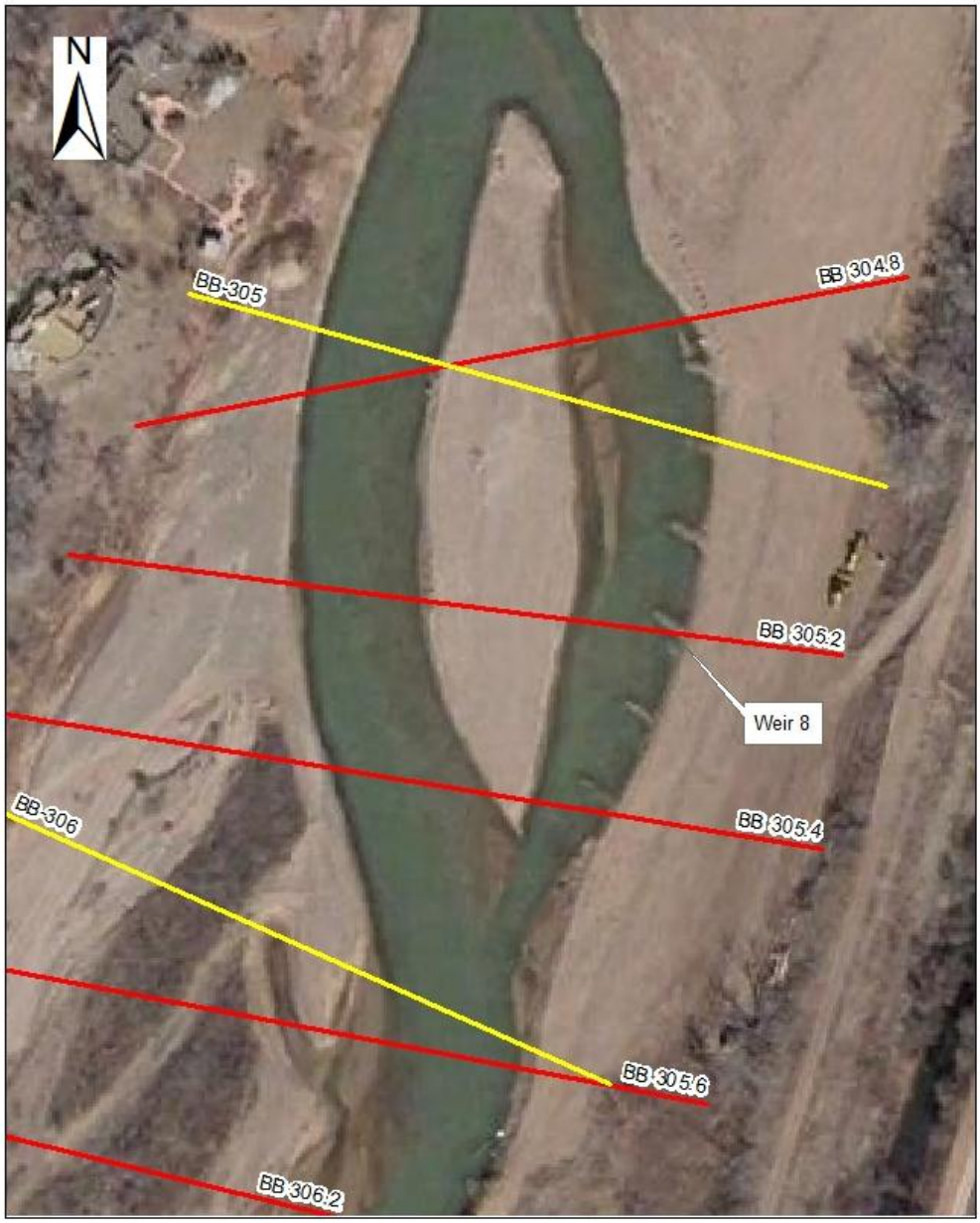

Figure 13. Cross-section survey locations in the weir field

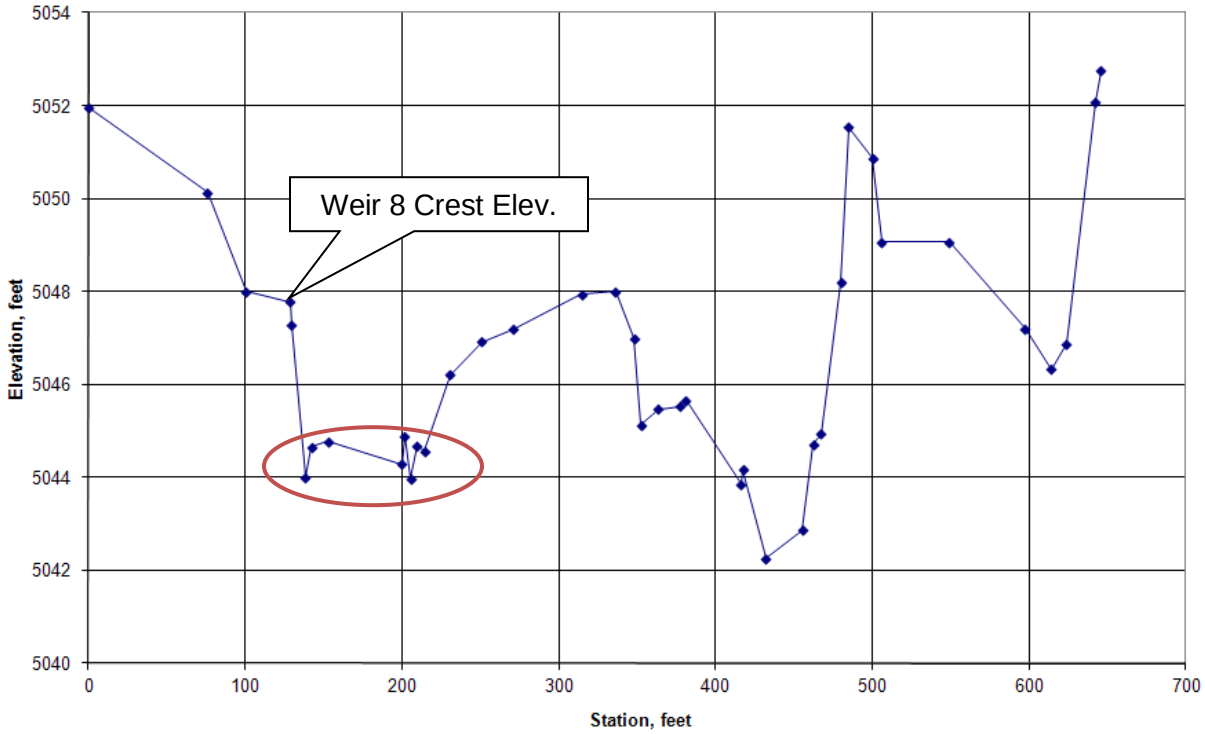

Figure 14. Survey of Cross Section BB 305.2 from 2007 (adapted from Bui (2011))

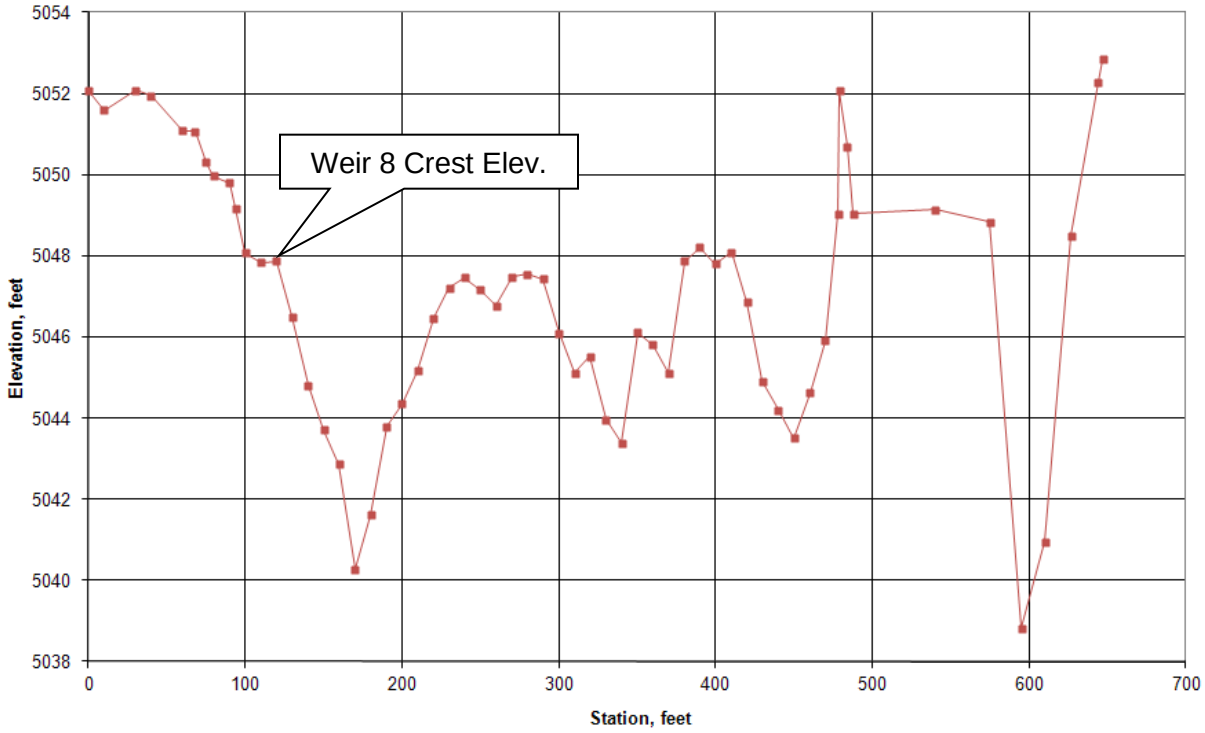

Figure 15. Survey of Cross Section BB 305.2 from 2008 (adapted from Bui (2011))

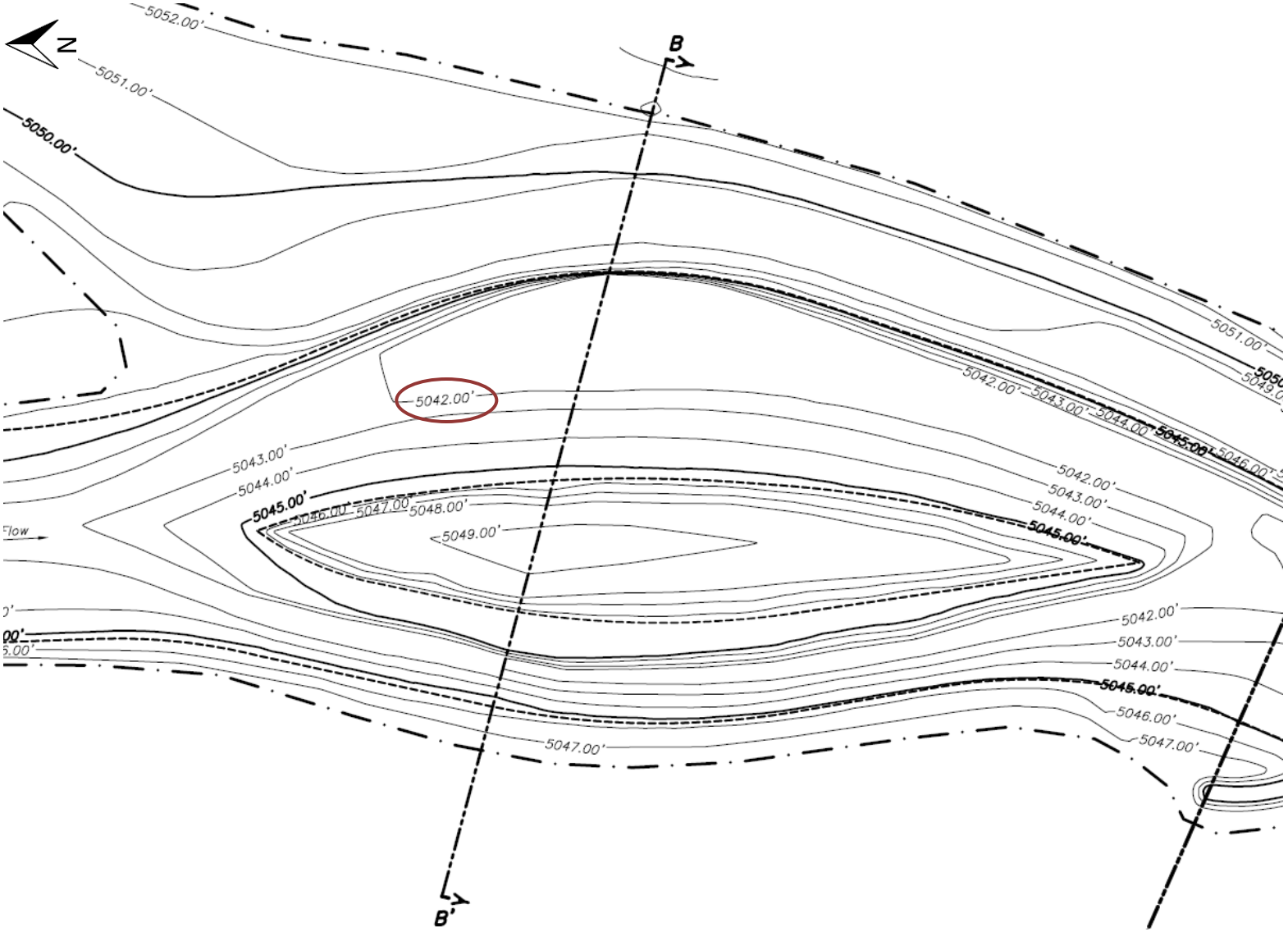

Figure 16. Final grading plan (adapted from BIO-WEST (2006))

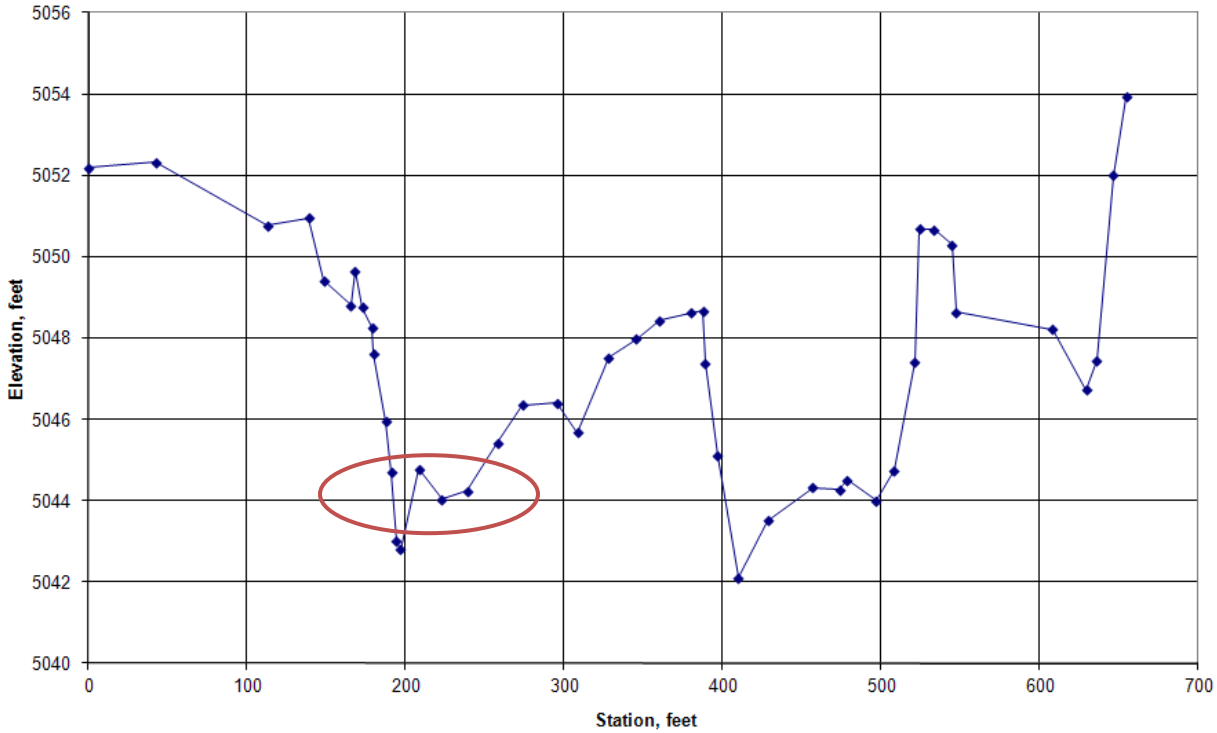

Figure 17. Survey of Cross Section BB 304.8 from 2007 (adapted from Bui (2011))

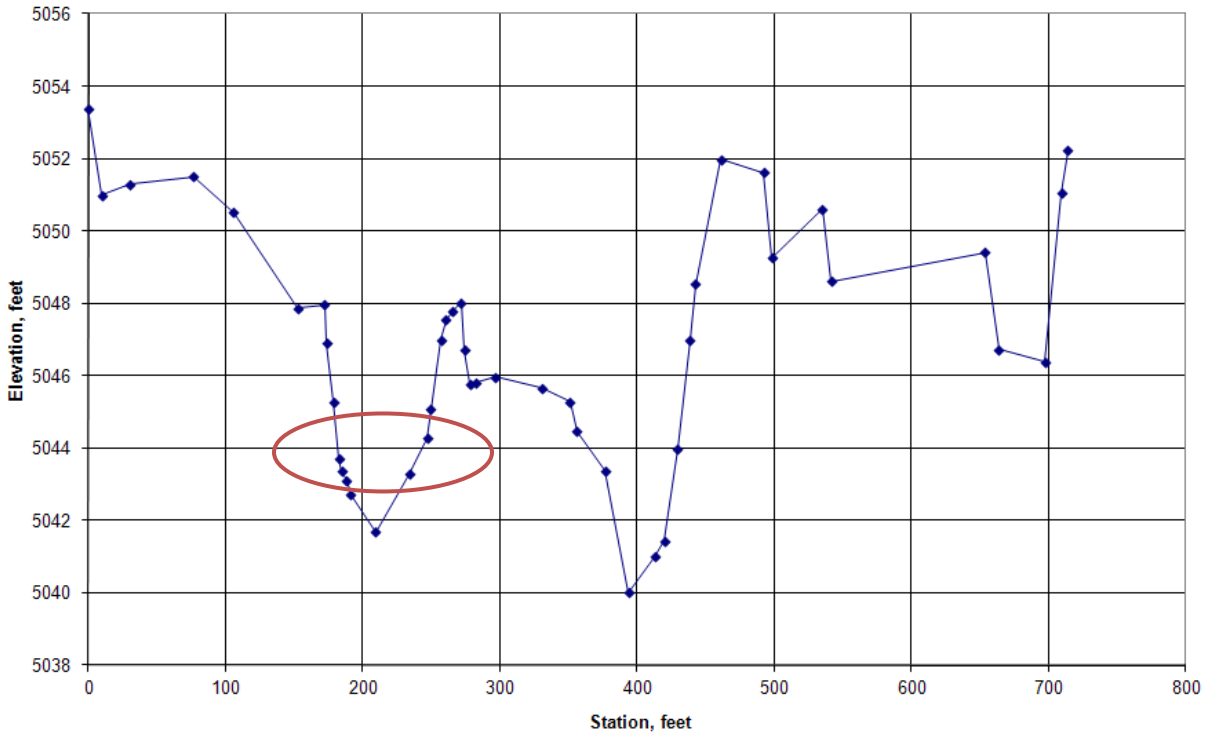

Figure 18. Survey of Cross Section BB 305.4 from 2007 (adapted from Bui (2011))

The post-construction channel planform was significantly modified from the pre-construction planform. For the physical model studies, no alterations were made in channel planform between baseline and weir field investigations. Therefore, the radius of curvature was determined using an aerial photograph taken after the channel realignment and weir-field construction to provide a suitable comparison. Figure 19 displays the radius of curvature superimposed on the February 25, 2007 aerial photograph. The radius of curvature was determined to be 675 ft.

Figure 19. Radius of curvature sketch

Discharge measurements were taken on May 16 of 2007 and May 22 and 23 of 2008. Table 5 provides a summary of discharge measurements and dates for discharge and flow-velocity measurements. Velocity data were not recorded on the same days as the discharge measurements, and the discharge measured on May 22 was 631 cfs greater than the discharge measured on May 23 of 2008, indicating the potential for significant changes in mean daily flow between consecutive days. Therefore, an analysis was conducted to estimate discharges for the dates of velocity data collection using the USGS Gaging Station 08329918 located on the Rio Grande 10.9 mi downstream from the Bernalillo Site at the Alameda Bridge. A linear interpolation scheme was developed to predict discharge at the Bernalillo Site ($Q_{Bern\text{-}Int}$) using a

known USGS discharge at the Alameda Bridge USGS Gage Station (Q_{Alam}) and calibrated using measured data from both locations on May 22 and 23 of 2008. Equation (6) provides the interpolation scheme:

$$Q_{Bern-Int} = 1.117 Q_{Alam} \tag{6}$$

Additionally, the Bernalillo Site discharge was estimated using known USGS discharges at the Alameda Bridge USGS Gage Station and available information on channel seepages in the Upper Middle Rio Grande. Channel seepage rates for the Upper Middle Rio Grande ($R_{seepage}$) are provided in Table 6 and range from approximately 6.3 to 7.4 cfs/mi for discharges ranging from 2,000 cfs to 5,000 cfs (S. S. Papadopulos and Associates, Inc. (SSPA) 2007, 2008). Wastewater outlets, various arroyos, and the Albuquerque Metropolitan Arroyo Flood Control Authority North Diversion Channel feed into the Rio Grande between the Bernalillo Field Site and the Alameda Bridge gauge. However, data were not available to compute their discharge contributions. The discharge at the Bernalillo Site was estimated as the Alameda Bridge discharge plus the computed seepage between the two sites. Equation (7) provides the expression used to compute the adjusted USGS discharge for the Bernalillo Site ($Q_{Bern-Adj}$):

$$Q_{Bern-Adj} = Q_{Alam} + (10.88 \text{ mi}) R_{seepage} \tag{7}$$

Computed discharges using both estimation techniques are provided in Table 5; and Figure 20 and Figure 21 show estimated and measured discharges versus dates for 2007 and 2008, respectively. As evidenced by Figure 20 and Figure 21, the interpolation technique presented in Equation (6) provided the best estimate of discharge compared to the measured discharges. Thus, discharges from the interpolation technique were used in the HEC-RAS model to evaluate baseline hydraulic conditions. Inaccuracy of the adjusted USGS discharge estimation technique compared to measured discharge is likely due to un-quantified outlet discharges that enter the reach between the two sites.

Table 5. Dates of velocity and discharge data collection, and measured and estimated discharges

Date (mm/dd/yyyy)	Data Collected	Bernalillo Measured Discharge (cfs)	Alameda Bridge USGS Gage Discharge (cfs)	Bernalillo Interpolated USGS Discharge (cfs)	Bernalillo Adjusted USGS Discharge (cfs)
5/14/2007	Velocity	n/a	2,500	2,237	2,571
5/16/2007	Discharge	2,102	2700[A]	2,416	2,772
5/19/2008	Velocity	n/a	3,320	2,971	3,395
5/20/2008	Velocity	n/a	3,290	2,944	3,365
5/21/2008	Velocity	n/a	3,360	3,007	3,435
5/22/2008	Discharge	3,626	4,040	3,616	4,117
5/23/2008	Discharge	4,257	4,770	4,269	4,850

[A]USGS estimated discharge
n/a = not available

Table 6. River seepage rates for the Upper Middle Rio Grande (SSPA 2007, 2008)

Discharge (cfs)	River Seepage (cfs/mi)
100	4.20
500	5.12
1,000	5.67
2,000	6.34
3,000	6.77
5,000	7.43
7,000	8.77
10,000	15.29

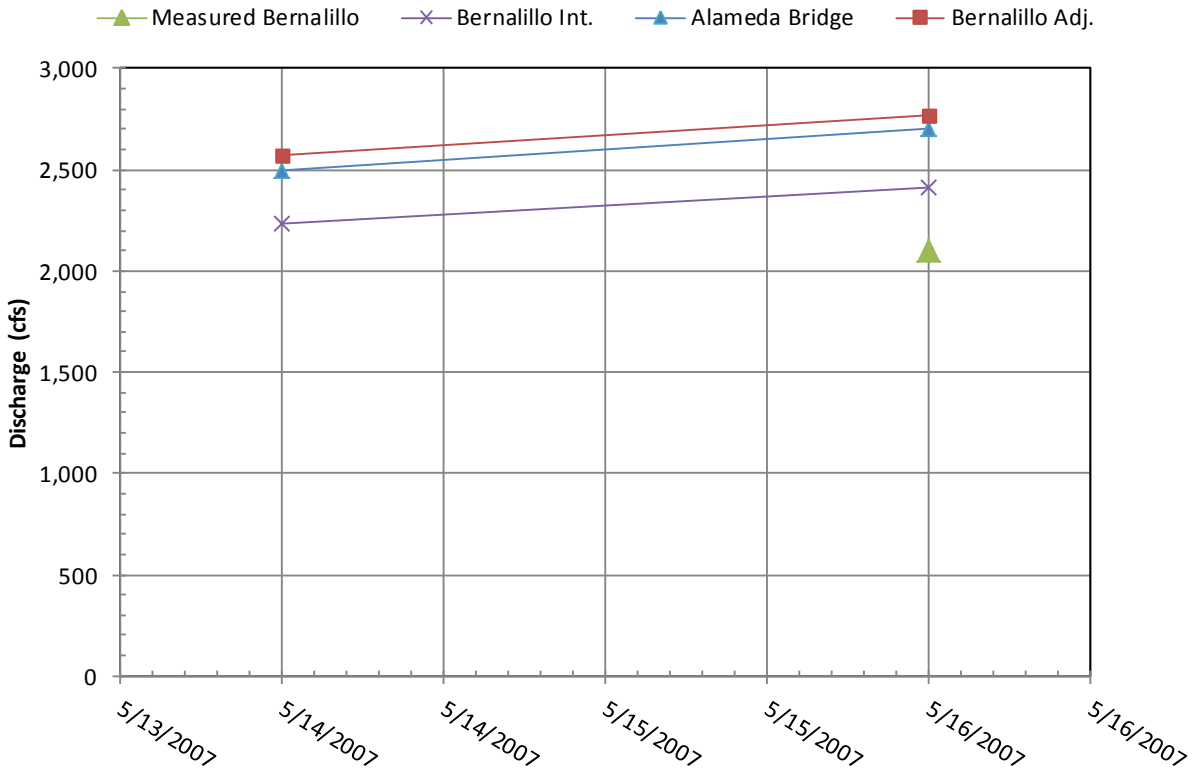

Figure 20. Discharge measurements and estimations from 2007

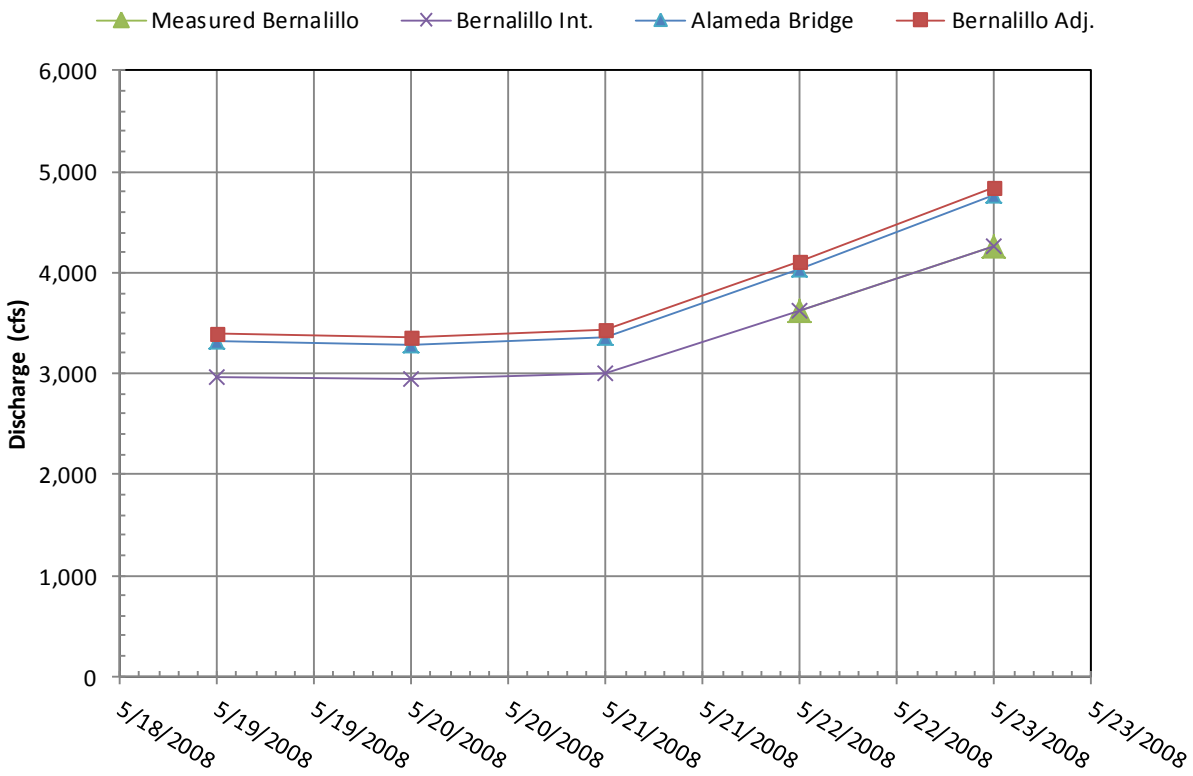

Figure 21. Discharge measurements and estimations from 2008

HEC-RAS Model and Results

A HEC-RAS model for the Bernalillo Site was developed by Reclamation's Albuquerque Area Office and provided to Colorado State University. Baseline flow velocities and other hydraulic parameters were determined using the Bernalillo Site HEC-RAS model with the estimated discharges associated with the velocity data-collection dates. The model was developed using 2008 and 2009 survey data calibrated and validated with observed water depths and discharges at two range lines, BB 303.7 and BB 304.8, collected on May 22 and 23 of 2008. Table 7 provides a summary of cross sections in the model including assigned Manning's roughness coefficients, which ranged from 0.050 at the downstream-most cross section to 0.020 at the upstream-most cross section. A HEC-RAS model for the pre-structure installation (baseline) condition would allow computation of necessary hydraulic parameters for computing *MVR* and *AVR* values. However, the Bernalillo HEC-RAS model was developed from post-construction cross sections, and measured discharges and water-surface elevations.

Table 7. HEC-RAS cross-section descriptions and Manning's roughness values

Description	River Station	Reach Length (ft)	Cumulative Channel Length (ft)	Manning's Roughness
BB 309	0	0	0	0.050
BB 306.6	1	986.73	986.73	0.045
Int. XS	1.2	37.27	1,024.00	0.040
Int. XS	1.4	37.27	1,061.27	0.030
Int. XS	1.6	37.27	1,098.54	0.025
Int. XS	1.8	37.27	1,135.81	0.025
BB 306.45	2	37.27	1,173.08	0.025
Int. XS	2.2	83.57	1,256.65	0.025
Int. XS	2.4	83.57	1,340.22	0.025
Int. XS	2.6	83.57	1,423.79	0.025
Int. XS	2.8	83.57	1,507.36	0.025
BB 305.6	3	83.57	1,590.93	0.025
BB 305.4	4	207.41	1,798.34	0.025
BB 305.2	5	156.66	1,955.00	0.025
BB 304.8[A]	6	267.83	2,222.83	0.020
BB 304	7	553.21	2,776.04	0.020
BB 303.7[A,B]	8	54.80	2,830.84	0.020

[A]used for calibration/validation
[B]used as the representative cross section for baseline conditions
Int. XS = cross section interpolated from surveyed cross sections

The Bernalillo Site HEC-RAS model was evaluated to determine a cross section to use as an approximation for baseline conditions. Given the high roughness values at the downstream end of the model, flow velocities computed from HEC-RAS in that area were generally less than the corresponding measured flow velocities within the weir field. Cross Section BB 303.7 was used as the representative cross section for baseline conditions because it was the upstream-most cross section, away from the influence of the downstream high roughness values, and potentially out of the hydraulic influence of the bendway-weir field. Additionally, Cross Section BB 303.7 was used for the calibration and validation, indicating that HEC-RAS hydraulic output data at that cross section matched well with measured data. However, it is important to note that Cross Section BB 305.2, located within the weir field, has two channels at the evaluated discharges and Cross Section BB 303.7 has only one channel for flow conveyance. Table 8 provides a summary of the HEC-RAS output for hydraulic parameters at Cross Section BB 303.7 for each of the evaluated discharges. Average cross-sectional flow velocity, maximum cross-section flow depth, water-surface elevation, flow area, and channel top width are included in Table 8. *MVR* and *AVR* values were calculated using the weir-crest elevation from Cross Section BB 305.2. Therefore, computed water-surface elevations for Cross Section BB 303.7 were adjusted to represent elevations at Cross Section BB 305.2. Each elevation was adjusted by 3.56 ft, which was determined from the difference in average bankfull elevation between the two cross sections.

Table 8. HEC-RAS hydraulic parameters for Cross Section BB 303.7

Discharge (cfs)	Average Flow Velocity (ft/s)	Maximum Flow Depth (ft)	WSE Cross Section BB 303.7 (ft)	Estimated WSE Cross Section BB 305.2 (ft)	Flow Area (ft^2)	Top Width (ft)
2,237	3.32	5.41	5,048.40	5,044.84	686	201
2,971	3.77	6.02	5,049.01	5,045.45	816	221
2,944	3.76	6.00	5,048.99	5,045.43	810	220

Analysis of Velocity Ratios for the Bernalillo Field Site

Maximum Velocity Ratios (*MVR*) and Average Velocity Ratios (*AVR*) were computed for the Bernalillo Field Site from bendway weir field velocity data and corresponding bendway-weir design parameters and channel hydraulic parameters. Geometric and hydraulic similarities exist between both the Bernalillo Site bendway weirs and the vanes and submerged spur dikes tested within the physical model. Specifically, each of the structures has a submerged component and both the vanes and the Bernalillo Site bendway weirs have sloped crests. Thus, design equations for the combined structure set, vanes, and submerged spur dikes were used to compute *MVR* and *AVR* values both along the outer-bank and centerline of the channel.

Initially, dimensionless parameters for each of the baseline hydraulic conditions were computed and compared to the dimensionless parameter ranges from the physical-model database from which the *MVR* and *AVR* equations were developed. Table 9 provides the computed dimensionless parameters for each baseline discharge; and Table 10 provides the dimensionless parameter ranges from the physical-model database. The L_{ARC}/T_W, $L_{W\text{-}PROJ}/T_W$, and D_{RATIO} dimensionless parameters computed for the Bernalillo Field Site were observed to be below the ranges of the laboratory database by a maximum of 32%, 24%, and 45%, respectively. Low values for L_{ARC}/T_W and $L_{W\text{-}PROJ}/T_W$ indicate weirs relatively short in length with a relatively large spacing between the structures; whereas, the low D_{RATIO} value indicates a low flow depth relative to the structure crest height. Values computed for A^*, R_C/T_W, and $2\theta/\pi$ were all within the bounds of the laboratory database.

Table 9. Dimensionless parameters computed for evaluated discharges

Discharge	A^*	L_{ARC}/T_W	R_C/T_W	$L_{W\text{-}PROJ}/T_W$	D_{RATIO}	$2\theta/\pi$ (rad)
2,237	12.8	0.373	3.35	0.117	0.631	0.778
2,971	10.7	0.339	3.06	0.106	0.702	0.778
2,944	10.8	0.341	3.07	0.107	0.700	0.778

Table 10. Dimensionless parameter ranges evaluated in the laboratory (from Scurlock *et al.* (2012b))

Structure Type	A^*		L_{ARC}/T_W		R_C/T_W		$L_{W\text{-}PROJ}/T_W$		D_{RATIO}		$2\theta/\pi$ (rad)	
	max	min	max	min	max	min	max	min	max	min	max	min
All data	27.00	10.75	3.085	0.547	6.862	2.479	0.373	0.140	6.984	0.768	1.000	0.667
Vane	19.40	10.75	2.299	0.547	6.862	2.479	0.373	0.146	6.984	1.135	1.000	0.667
Spur-dike	27.00	10.75	3.085	0.578	6.862	2.620	0.317	0.150	1.000	0.768	1.000	0.667
Submerged Spur Dike	27.00	10.75	2.596	0.547	5.775	2.479	0.267	0.140	1.182	1.154	1.000	0.667

max = maximum, min = minimum

MVR and *AVR* values were predicted for the Bernalillo Site along the channel centerline and outer-bank using Equation (3) and coefficients presented in Table 1 for all structures, vanes, and submerged spur dikes. Table 11 provides the predicted *MVR* and *AVR* values in addition to the observed *MVR* and *AVR* values computed from the field velocity measurements and HEC-RAS baseline velocity data. Additionally, observed and predicted velocity ratios versus discharge for MVR_o, AVR_o, MVR_c, and AVR_c, are shown in Figure 22, Figure 23, Figure 24, and Figure 25, respectively.

Table 11. Observed and predicted *MVR* and *AVR* values using Equation (3)

Outer-bank MVR Values

Discharge (cfs)	$V_{Ave\ Baseline}$ (ft/s)	Observed MV_o (ft/s)	Observed MVR_o	Predicted $MVR_{o\ -\ ALL\ TYPES}$	Predicted $MVR_{o\ -\ SUB.\ SPUR\ DIKE}$	Predicted $MVR_{o\ -\ VANE}$
2,237	3.32	2.51	0.76	0.41	2.50	9.02
2,971	3.77	3.07	0.81	0.50	2.62	7.28

Outer-bank AVR Values

Discharge (cfs)	$V_{Ave\ Baseline}$ (ft/s)	Observed AV_o (ft/s)	Observed AVR_o	Predicted $AVR_{o\ -\ ALL\ TYPES}$	Predicted $AVR_{o\ -\ SUB.\ SPUR\ DIKE}$	Predicted $AVR_{o\ -\ VANE}$
2,237	3.32	2.04	0.61	0.15	0.36	0.87
2,971	3.77	2.57	0.68	0.16	0.41	0.68

Centerline MVR Values

Discharge (cfs)	$V_{Ave\ Baseline}$ (ft/s)	Observed MV_c (ft/s)	Observed MVR_c	Predicted $MVR_{c\ -\ ALL\ TYPES}$	Predicted $MVR_{c\ -\ SUB.\ SPUR\ DIKE}$	Predicted $MVR_{c\ -\ VANE}$
2,237	3.32	4.84	1.46	1.27	1.16	1.63
2,944	3.76	4.35	1.16	1.21	1.11	1.53

Centerline AVR Values

Discharge (cfs)	$V_{Ave\ Baseline}$ (ft/s)	Observed AV_c (ft/s)	Observed AVR_c	Predicted $AVR_{c\ -\ ALL\ TYPES}$	Predicted $AVR_{c\ -\ SUB.\ SPUR\ DIKE}$	Predicted $AVR_{c\ -\ VANE}$
2,237	3.32	4.76	1.43	1.24	1.16	1.49
2,944	3.76	4.09	1.09	1.20	1.12	1.41

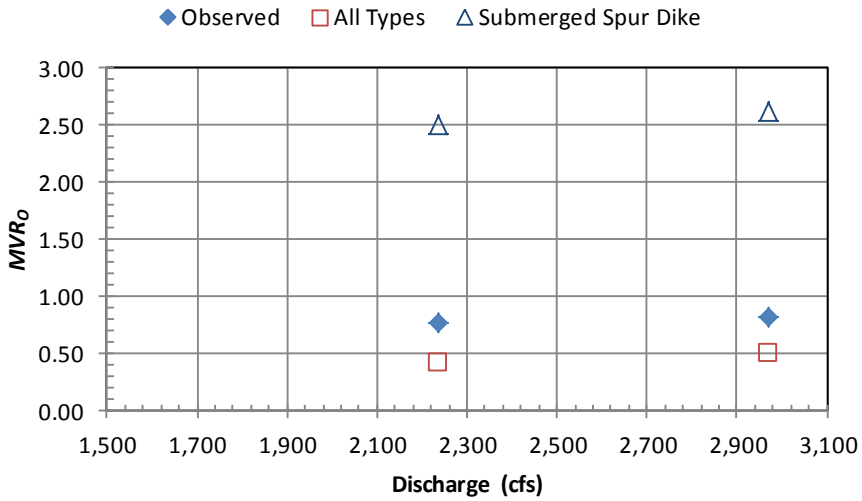

Figure 22. Observed and predicted MVR_o versus discharge for Equation (3) (vane results not shown)

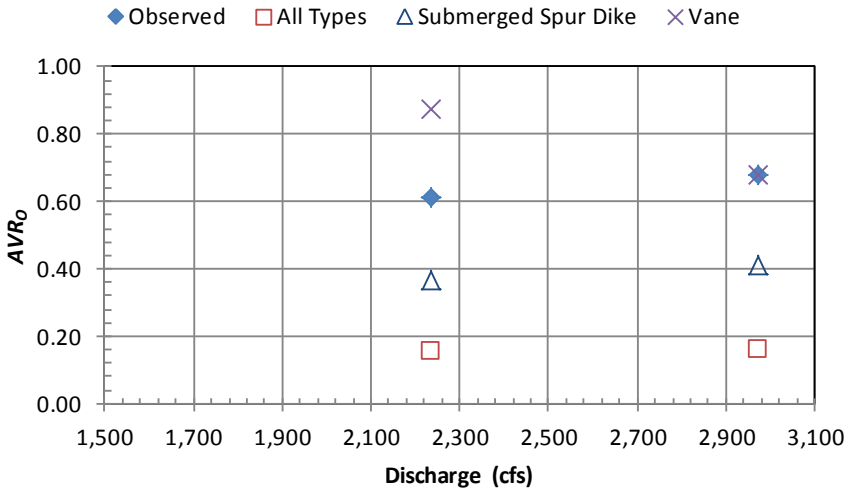

Figure 23. Observed and predicted AVR_o versus discharge for Equation (3)

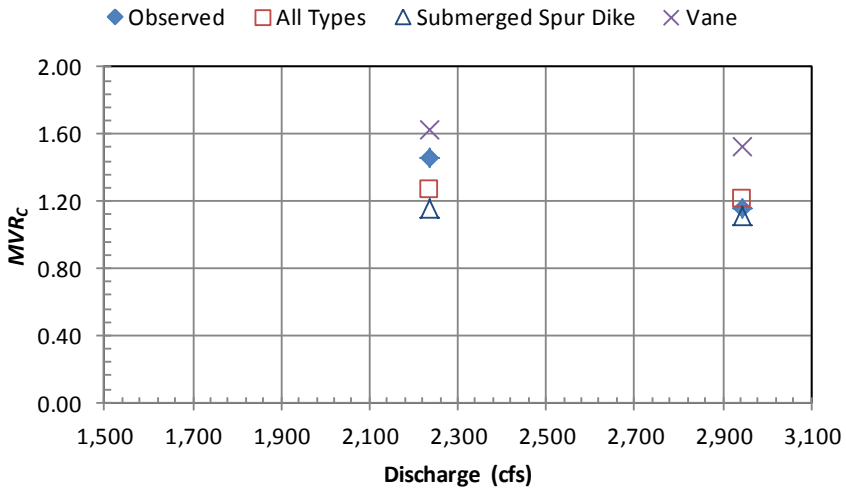

Figure 24. Observed and predicted MVR_c versus discharge for Equation (3)

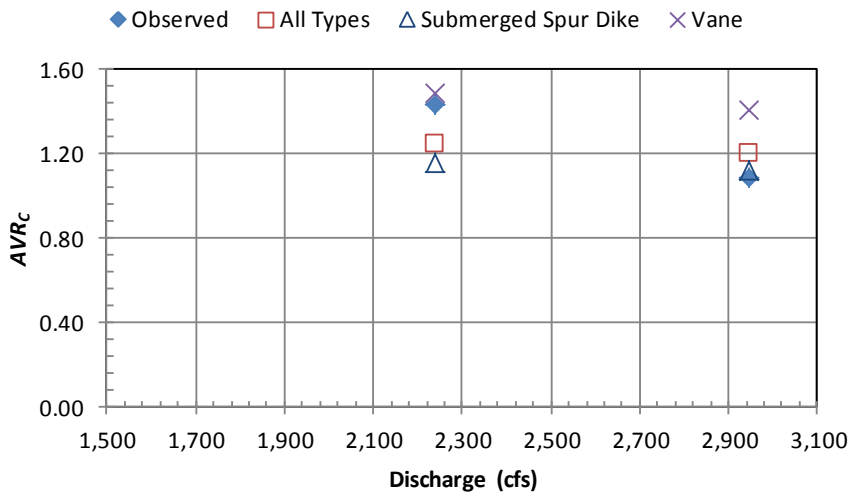

Figure 25. Observed and predicted AVR_c versus discharge for Equation (3)

The high MVR_o values computed from both the submerged spur dike and vane coefficients are attributed in part by dimensionless parameters being outside the bounds of the laboratory dataset. The equations were evaluated using the lower bounds of the dataset for the submerged spur dike and vane MVR_o equations provided in Table 10. The resulting MVR_o values were computed as 0.56 and 1.88 for the submerged spur dike equation and vane equation, respectively. Further analysis was conducted for the vane equation using the average of the minimum and maximum dimensionless parameters from the vane laboratory dataset. The MVR_o was computed as 0.30 using the average of the minimum and maximum dimensionless parameters, which is a reasonable value. Further sensitivity analysis of dimensionless parameters is recommended for assessing the ultimate bounds of the vane MVR_o equation. All other velocity ratios are within reasonable tolerances where outer-bank velocity ratios are less than one and centerline velocity ratios are greater than one. The submerged spur dike coefficients were collectively the best predictor for AVR_o, MVR_c, and AVR_c; and the equation using the all-structures coefficients was the best predictor for MVR_o. Additionally, all *MVR* values were greater than the corresponding *AVR* values, with the exception of the centerline submerged spur dike values, which is a good indicator of the robustness of the suite of equations. Further, large differences between the submerged spur dike MVR_c and AVR_c values were not observed as the values were nearly identical.

MVR_o values were also predicted for the Bernalillo Site using the Scurlock *et al.* (2012a) best-fit regression, Equation (4), and envelope regression, Equation (5). Table 12 provides the predicted best-fit and envelope MVR_o values in addition to the observed MVR_o values computed from the field velocity measurements and HEC-RAS baseline velocity data. Figure 26 shows the observed and predicted velocity ratios versus discharge. The best-fit regression equation under predicted the observed maximum outer-bank velocity ratios with an average percent error of 30%, and the envelope regression slightly under predicted the values with an average percent error of 8%.

Table 12. Observed and predicted best-fit and envelope MVR_o using Equation (4) and Equation (5)

Discharge (cfs)	$V_{Ave\ Baseline}$ (ft/s)	Observed MV_o (ft/s)	Observed MVR_o	Predicted $MVR_{o-EQ.4}$	Predicted $MVR_{o-ENVELOPE}$
2,237	3.32	2.51	0.76	0.51	0.68
2,971	3.77	3.07	0.81	0.59	0.77

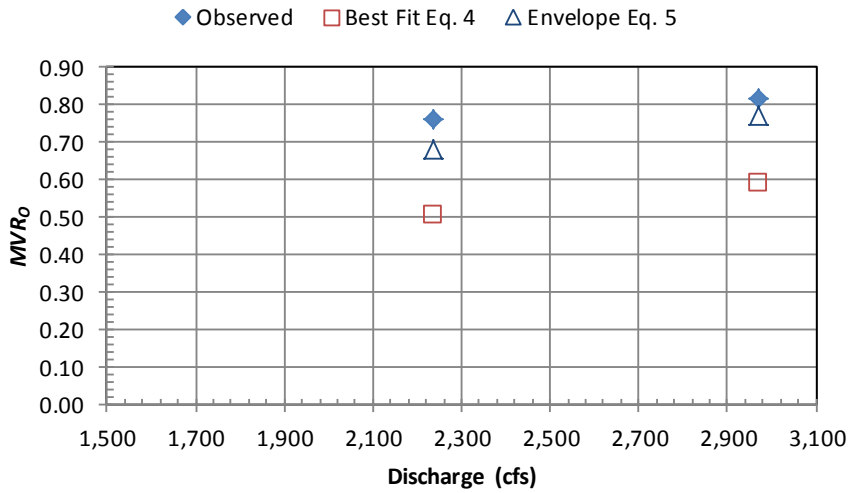

Figure 26. Observed and predicted MVR_o versus discharge for Equation (4) and Equation (5)

Discussion and Recommendations

There are two primary differences between the laboratory conditions under which the Scurlock *et al*. (2012b) velocity-ratio equations were developed and the Bernalillo field site. The laboratory physical model had a prismatic, trapezoidal channel, while the Bernalillo field site had a native-topography channel. Secondly, the Bernalillo site incorporated bendway-weir transverse features, and the transverse features evaluated in the physical model included only spur dikes and vanes. Both of these discrepancies induce uncertainty in the comparison of measured velocity ratios to predicted velocity ratios.

Furthermore, some of the available field data were not collected for the specific purpose of evaluating velocity-ratio equations. As a result, there were limitations in field data and a number of assumptions used to complete the analysis. Discharge measurements were not collected on the same days as the velocity measurements, resulting in the need to estimate discharge for the dates of velocity data collection. Further, limited weir-field velocity data were collected in 2008 and included only three velocity measurement locations suitable for the velocity-ratio analysis. The lack of baseline channel geometry data and corresponding hydraulic conditions induces the most uncertainty in the analysis. This deficiency resulted in using a representative cross section located upstream of the weir field and required that water-surface elevations be adjusted for comparison to weir-crest elevations. However, having a pre-construction HEC-RAS model may not have been suitable for evaluating the required baseline conditions given the significant alteration in planform between the pre- and post-construction site. Finally, the lack of survey data for weir-crest elevations following installation required

crest elevations to be estimated from one post-construction cross-section survey and the final bendway-weir design specification, which was in contradiction with the final site grading plan. Each of these factors contributes uncertainty to the computed *MVR* and *AVR* values from field measurements. Additional field-data collection specifically designed to capture comprehensive information for assessing velocity-ratio equations is recommended.

A comprehensive analysis of the Scurlock *et al.* (2012b) velocity-ratio equations was conducted and many positive aspects of the method were identified, in addition to potential areas for further assessment. Despite limited field data, all required parameters to compute velocity ratios could be determined. Further, twenty of the twenty-four total computed velocity ratios were within reasonable ranges regardless of multiple dimensionless parameters falling outside the bounds of the laboratory dataset; and nearly all computed *MVR* values were greater than corresponding *AVR* values, indicating continuity between the set of prediction equations. High MVR_o values were observed using the vane coefficients, which could not be contributed exclusively to dimensionless parameters being outside of the laboratory bounds. Therefore, further analysis is recommended to assess the ultimate bounds of the vane MVR_o equation.

Summary and Conclusions

In-stream transverse features were identified by Reclamation as potential solutions to channel instability in the Middle Rio Grande downstream of Cochiti Dam. In 2007, Reclamation constructed a series of bendway weirs to mitigate lateral channel migration at the Bernalillo Priority Site of the Middle Rio Grande in New Mexico. In 2007 and 2008, flow-velocity measurements within the Bernalillo Priority Site weir field were collected in addition to cross-section surveys and discharge measurements. A suite of empirical equations to predict changes in flow velocities along the centerline, inner-bank, and outer-bank of a channel bend for different types of transverse structures was developed by Scurlock *et al.* (2012b). This study utilized the Bernalillo field data to assess the velocity equations developed by Scurlock *et al.* (2012b).

Parameters for computing *MVR* and *AVR* values at the Bernalillo Site were obtained from field data, the final design report and drawings, and aerial photographs. Representative baseline flow velocities and other hydraulic parameters were computed using a HEC-RAS model of the Bernalillo Site. Velocity field data from Bui (2011) and ADV data collected in 2008, provided by the Bureau Technical Service Center, were used for evaluating the velocity-ratio prediction equations.

Dimensionless parameters for each of the baseline hydraulic conditions were computed and compared to the bounds of the physical-model database from which the velocity-ratio equations were developed. The L_{ARC}/T_W, $L_{W\text{-}PROJ}/T_W$, and D_{RATIO} dimensionless parameters computed for the Bernalillo Field Site were observed to be below the ranges for the laboratory database. Velocity ratios were predicted for the Bernalillo Site along the channel centerline and outer-bank using the Scurlock *et al.* (2012b) equations for all structures, vanes, and submerged spur dikes. The submerged spur dike coefficients were collectively the best predictor for AVR_o, MVR_c, and AVR_c; and the equation using the all-structures coefficients was the best predictor for MVR_o. Twenty of the twenty-four total computed velocity ratios were within expected ranges regardless of multiple dimensionless parameters falling outside the bounds of the laboratory dataset; and nearly all computed *MVR* values (83%) were greater than corresponding *AVR* values, indicating continuity between the set of prediction equations.

There were field-data limitations and multiple assumptions used to complete the analysis, which contribute to uncertainty in the computed velocity ratios. Despite field-data limitations, the assessment of the *MVR* and *AVR* equations was productive and identified that the required inputs could be easily attainable from a transverse-feature design. To provide a highly quantitative assessment of the Scurlock *et al.* (2012b) velocity-ratio prediction methods, a field study specifically designed to capture information for assessing the velocity-ratio equations is recommended.

References

Baird, D.C. (2012). "Bernalillo River Maintenance Project Bendway Weir Acoustic Doppler Velocity Meter 2008 Data, Middle Rio Grande Project, New Mexico, Upper Colorado Region." Department of the Interior, Bureau of Reclamation, Technical Service Center, Denver, CO., Report No.: SRH-2012-26.

BIO-WEST (2005). "Middle Rio Grande Project, Bernalillo Priority Site, Final Design Report." USBR Contract No. 03-CA-50-8007, Bureau of Reclamation, Albuquerque Area Office, Albuquerque, NM.

BIO-WEST (2006). "Bernalillo Priority Site: Final Design, Final Design Drawings." Bureau of Reclamation, Albuquerque Area Office, Albuquerque, NM.

Buchanan, T. J., and Somers, W. P. (1969). "Techniques for water resources investigations of the United States Geological Survey." Book 3, Applications of Hydraulics, Chapter 8.

Bui, C. (2011). "Bernalillo 2007 & 2008 Data Collection Report." Bureau of Reclamation, Albuquerque Area Office, Albuquerque, NM.

Darrow, J. D. (2004). "Effects of Bendway Weir Characteristics on Resulting Flow Conditions." M. S. Thesis, Colorado State University, Department of Civil Engineering, Fort Collins, CO.

Davinroy, R. D., Rapp, R. J., and Myhre R. E. (1998). "Hydroacoustic study of fishes in bendway weir fields of the Middle Mississippi River." In: Engineering Approaches to Ecosystem Restoration, Proceedings of the ASCE 1998 Wetlands Engineering and River Restoration Conference (D. F. Hayes, Ed.), Denver, CO, March 22-27, pp. 890–895.

Derrick, D. L. (1998). "Four years later, Harland Creek Bendway Weir/Willow Post Bank Stabilization Demonstration Project." In: Water Resources Engineering '98, Proceedings of the International Water Resources Engineering Conference (S. R. Abt, J. Young-Pezeshk, C. C. Watson, Eds.), Part 1 (of 2), Memphis, TN, August 3–7.

Heintz, M. L. (2002). "Investigation of Bendway Weir Spacing." M. S. Thesis, Colorado State University, Department of Civil Engineering, Fort Collins, CO.

Radspinner, R. R., Diplas, P., Lightbody, A. F., and Sotiropoulos, F. (2010). "River training and ecological enhancement potential using in-stream structures." *J. Hydraul. Eng.*, 136(12):967–980.

Richard, G. A. (2001). "Quantification and Prediction of Lateral Channel Adjustments Downstream from Cochiti Dam, Rio Grande, NM." Ph.D. Dissertation, Colorado State University, Department of Civil Engineering, Fort Collins, CO.

Schmidt, P. G. (2005). "Effects of Bendway Weir Field Geometry Characteristics on Channel Flow Conditions." M. S. Thesis, Colorado State University, Department of Civil Engineering, Fort Collins, CO.

Scurlock, S.M., Cox, A.L., Baird, D.C., and Thornton, C.I. (2012a). "Middle Rio Grande physical modeling – Instream structure analysis: Maximum outer-bank velocity reduction within the prismatic channel." Colorado State University, Department of Civil and Environmental Engineering. Fort Collins, CO.

Scurlock, S. M., Cox, A. L., Baird, D. C., Thornton, C. I., and Abt, S. R. (2012b). "Middle Rio Grande physical modeling – Instream transverse structure analysis: Maximum and average velocity ratios within the prismatic channel." Colorado State University, Department of Civil and Environmental Engineering, Fort Collins, CO.

Shields, Jr., F. D. (1983). "Design of habitat structures for open channels." *J. Water Resour. Plann. Manage*., 109(4):331–344.

Shields, Jr., F. D., Knight, S. S., and Cooper, C. M. (1998). "Addition of spurs to stone toe protection for warmwater fish habitat." *J. Am. Water Resour. Assoc.*, 34(6):1427–1436.

Sixta, M. and Nemeth, M. (2005). "Bernalillo Priority Site Project Description." Bureau of Reclamation, Albuquerque Area Office, Albuquerque, NM.

SSPA. (2007). "Riparian Groundwater Models for the Middle Rio Grande: ESA Collaborative Program FY07, Model Refinement." S. S. Papadopulos and Associates, Inc. and New Mexico Interstate Stream Commission, Boulder, CO.

SSPA. (2008). "Riparian Groundwater Models for the Middle Rio Grande: ESA Collaborative Program FY08, Model Refinement." S. S. Papadopulos and Associates, Inc. and New Mexico Interstate Stream Commission, Boulder, CO.